Journal of Controlled Release 349 (2022) 954–962

Contents lists available at ScienceDirect

Journal of Controlled Release

journal homepage: www.elsevier.com/locate/jconrel

Magnetic beads for the evaluation of drug release from biotinylated polymeric micelles in biological media

Yan Wang [a], Marcel H. Fens [a], Nicky C.H. van Kronenburg [b], Yang Shi [c], Twan Lammers [c], Michal Heger [a,d], Cornelus F. van Nostrum [a], Wim E. Hennink [a,*]

[a] Department of Pharmaceutics, Utrecht Institute for Pharmaceutical Sciences, Utrecht University, Universiteitsweg 99, 3508 TB Utrecht, the Netherlands
[b] Department of Translational Neuroscience, University Medical Center Utrecht Brain Center, Universiteitsweg 100, 3584 CG Utrecht, the Netherlands
[c] Department of Nanomedicine and Theranostics, Institute for Experimental Molecular Imaging, RWTH Aachen University Clinic, Forckenbecktrasse 55, 52074 Aachen, Germany
[d] Department of Pharmaceutics, Jiaxing Key Laboratory for Photonanomedicine and Experimental Therapeutics, College of Medicine, Jiaxing University, Jiaxing 314001, Zhejiang, PR China

ARTICLE INFO

Keywords:
Drug release
Polymeric micelles
Biotin
Streptavidin-coated magnetic beads

ABSTRACT

To improve the reliability of *in vitro* release studies of drug delivery systems, we developed a novel *in vitro* method for the evaluation of drug release from polymeric micelles in complex biological media. Polymeric micelles based on poly(*N*-2-hydroxypropyl methacrylamide)-*block*-poly(*N*-2-benzoyloxypropyl methacrylamide) (p(HPMAm)-b-p(HPMAm-Bz)) of which 10% of the chains was functionalized with biotin at the p(HPMAm) terminus were prepared using a solvent extraction method. The size of the micelles when loaded with a hydrophobic agent, namely paclitaxel (a clinically used cytostatic drug) or curcumin (a compound with multiple pharmacological activities), was around 65 nm. The biotin decoration allowed the binding of the micelles to streptavidin-coated magnetic beads which occurred within 10 min and reached a binding efficiency of 90 ± 6%. Drug release in different media was studied after the magnetic separation of micelles bound to the streptavidin-coated beads, by determination of the released drug in the media as well as the retained drug in the micellar fraction bound to the beads. The *in vitro* release of paclitaxel and curcumin at 37 °C in PBS, PBS containing 2% v/v Tween 80, PBS containing 4.5% *w/v* bovine serum albumin, mouse plasma, and whole mouse blood was highly medium-dependent. In all media studied, paclitaxel showed superior micellar retention compared to curcumin. Importantly, the presence of serum proteins accelerated the release of both paclitaxel and curcumin. The results presented in this study show great potential for predicting drug release from nanomedicines in biological media which in turn is crucial for their further pharmaceutical development.

1. Introduction

Polymeric micelles are widely investigated for their potential to incorporate a wide range of poorly water-soluble drugs to improve safety and therapeutic efficacy [1–4], and several formulations have been approved for clinical use in cancer therapy, *e.g.*, the Cremophor-free based formulation of paclitaxel, in particular, Genexol-PM and Apealea [5]. Polymeric micelles are appreciated to *i)* protect the encapsulated drug against degradation and metabolic conversion upon administration, *ii)* prolong blood circulation and tumor accumulation, *iii)* release the drug in a sustained and controlled manner at specific systemic sites, and ultimately, *iv)* increase the therapeutic index of hydrophobic drugs. *In vitro* stability and drug release studies (also called dissolution kinetics) are key parameters in the (pre-)clinical evaluation of nanomedicines.

Present drug release assays for nanocarriers are commonly performed using separation or dialysis methods [6–8]. In the separation method, nanoparticles are dispersed in release media and incubated under constant agitation at physiological temperature. The media with the released drug are subsequently separated from the nanoparticles using centrifugation, size-exclusion chromatography (SEC), or field-flow fractionation (FFF). However, the complete separation of the nano-sized particles from the release media is challenging, particularly in complex media such as blood, leading to inaccurate determination of the released

* Corresponding author.
E-mail address: W.E.Hennink@uu.nl (W.E. Hennink).

https://doi.org/10.1016/j.jconrel.2022.07.044
Received 10 June 2022; Received in revised form 22 July 2022; Accepted 31 July 2022
Available online 9 August 2022

drugs. In the dialysis method, nanoparticles are transferred into a dialysis bag containing a certain release medium. The nanoparticles are retained in the dialysis bag, whereas the released drug diffuses through the dialysis membrane to the external phase containing the same release medium that is frequently sampled for quantitative analysis of the drug concentration. The dialysis membrane itself functions as a diffusion barrier, however, precipitation of released drugs in the bag and adsorption to the bag may occur. Consequently, the amount of drug determined in the bulk solution does not properly reflect the release profile of the investigated nanoformulation [9,10].

Besides the type of release assay, the selection of appropriate release media is also an important consideration. Phosphate buffered saline (PBS) is the most used medium for drug release studies. However, to maintain sink conditions, defined as the volume of the selected medium which can dissolve at least three to ten times the amount of drugs present in the dosage form [11], an exceedingly large volume of buffer or addition of surfactants is required to solubilize the released hydrophobic drugs. The former makes drug quantification difficult due to the low concentration [12], and the latter might destabilize polymeric micelles resulting in misleading release profiles [13,14]. Moreover, the mentioned *in vitro* assays fail to predict *in vivo* retention due to the complexity of the physiological media such as plasma and blood. For instance, the presence of plasma proteins and cells or the formation of the protein corona might act as a sink or barrier for the released drug [15–20].

In the present study, a novel *in vitro* assay based on biotin-streptavidin interaction was developed and validated. Biotinylated polymeric micelles loaded with paclitaxel and curcumin were employed for evaluation of their release properties in different media. Micelles based on poly(*N*-2-hydroxypropyl methacrylamide)-*block*-poly(*N*-2-benzoyloxypropyl methacrylamide) (p(HPMAm)-b-p(HPMAm-Bz)) were selected because of their good stability and drug loading capacity [21,22]. Biotin, also known as vitamin B7, binds to biotin receptors, which are (over)expressed by certain cells, such as lung cancer cells [23], and when decorated on the micelle surface, it can thus potentially be used as a targeting ligand. Moreover, biotin binds to the protein streptavidin with high affinity [23]. Therefore, in the present study, this strong interaction was exploited to capture drug-loaded biotinylated micelles from media (from PBS to whole mouse blood) using streptavidin-coated magnetic beads. This method allows determining simultaneously both the amount of drug released in the different media as well as the amount of drug still retained in the micelles. Overall, this study aimed to validate the novel *in vitro* release method based on biotinylated polymeric micelles loaded with paclitaxel and curcumin using streptavidin-coated magnetic beads to get insights into the drug retention capability of micelles in biological fluids.

2. Materials and methods

2.1. Materials

Streptavidin-coated magnetic beads (cat# BM551) dispersed in phosphate-buffered saline (pH = 7.5) containing 0.1% bovine serum albumin with EDTA and sodium azide were purchased from Bangs labs (Fishers, IN, USA). The characteristics are given by the supplier as follows, mean diameter = 1.5 μm, binding capacity = 2 μg biotin per 1 mg beads, and particle concentration = 5 mg/mL. Paclitaxel (PTX, cat# P9600) was supplied by LC labs (Woburn, MA, USA). Curcumin (cat# C7727), bovine serum albumin (BSA, cat# A7030, fatty acid-free), and HEPES (4-(2-hydroxyethyl)-1-piperazineethanesulfonic acid, cat# H7006) were purchased from Sigma-Aldrich (Zwijndrecht, the Netherlands), and dimethylformamide (DMF, cat# 041933) and acetonitrile (ACN, cat# 012013) were from Biosolve (Valkenswaard, the Netherlands). RC membrane syringe filters (0.45 μm, cat# AF0–2123-51) were supplied by Phenomenex (Utrecht, the Netherlands). Magnetic rack (DynaMag-2 Magnet, cat# 12321D), Spectra/Por dialysis membrane (MW 6–8 kDa, cat# 11495839), and phosphate-buffered saline (PBS, pH = 7.4, containing 11.9 mM phosphate, 137 mM sodium chloride, and 2.7 mM potassium chloride, cat# BP2438–20) were purchased from Thermo Fisher Scientific (Landsmeer, the Netherlands). Polysorbate 80 (Tween 80, cat# T164–500) was ordered from Fisher Scientific (Loughborough, Leicestershire, UK). Block copolymers p(HPMAm)-b-p(HPMAm-Bz) with or without biotin conjugated to the p(HPMAm) terminus, as well as Cy3-labeled block copolymers, were synthesized and characterized as previously reported (characteristics given in Table S1) [21]. Mouse blood from C57BL/6 J mice was collected into EDTA-containing (0.184 M) tubes and plasma was prepared by centrifugation at 1000 *g* for 15 min at 4 °C.

2.2. Preparation and characterization of biotinylated polymeric micelles

Empty biotinylated p(HPMAm)-b-p(HPMAm-Bz) micelles co-labeled with Cy3 were prepared by a solvent extraction method [21]. In detail, 20 mg of polymers, comprising nonbiotinylated polymer (entry 1 in Table S1), biotinylated polymer (0, 2.5, 5, 10, 15, and 20%, respectively; entry 2 in Table S1) and Cy3-labeled polymer (2.5%; entry 3 in Table S1) were dissolved in 1 mL of DMF. Subsequently, the polymer solution was transferred into 1 mL of Milli-Q water while stirring for 1 min. DMF was subsequently removed by dialysis in a Spectra/Por dialysis membrane with a molecular weight cutoff of 6–8 kDa followed by filtration through a 0.45 μm RC membrane syringe filter.

Drug-loaded biotinylated p(HPMAm)-b-p(HPMAm-Bz) micelles were prepared using the same method as for the empty micelles. In brief, 18 mg of nonbiotinylated polymer (entry 1 in Table S1), 2 mg of biotinylated polymer (entry 2 in Table S1), and drug (0.6 or 2 mg of PTX, or 2 mg of curcumin) were dissolved in 1 mL DMF. Micelles were formed and dialyzed as described above for empty micelles.

The size of the obtained biotinylated polymeric micelles was determined by dynamic light scattering (DLS) after 10-fold dilution in water at 25 °C using a Zetasizer Nano S 173 (Malvern Instruments, Malvern, Worcestershire, UK). The *Z*-average diameter (Z_{ave}) and polydispersity index (PDI) were calculated by the Zetasizer software v.7.13. The zeta-potential of the biotinylated micelles was measured after 10-fold dilution in 10 mM HEPES buffer, pH = 7.4, using a Zetasizer Nano Z (Malvern Instruments).

To determine the amount of the loaded drug, the micellar aqueous dispersions were diluted 10-fold with ACN to destabilize the micelles, and the dissolved PTX or curcumin was subsequently quantified by HPLC (Waters Alliance System). HPLC methods for the detection and quantification of these two compounds can be found in section 1 of the Supporting Information (SI). The encapsulation efficiency (EE) and loading capacity (LC) were calculated by the following formulas:

$$EE(\%) = \frac{\text{weight of loaded drug}}{\text{weight of drug used for loading}} \times 100\%$$

$$LC(\%) = \frac{\text{weight of loaded drug}}{\text{weight of loaded drug} + \text{weight of loaded polymer}} \times 100\%.$$

The concentration of the micelles was measured by thermogravimetric analysis (TGA) using a TA instrument Q50 (Waters, Milford, MA, USA). In detail, 50 μL of homogenized micelle dispersion was transferred into a tared aluminum pan, followed by heating from 20 to 120 °C at 20 °C/min with an isothermal hold time of 100 min. The maximum temperature was far below the degradation temperature of PTX (220 °C) and curcumin (180 °C) [24,25]. A sample of dry polymer, analyzed for comparison, displayed no mass loss, indicating the stability of p(HPMAm)-b-p(HPMAm-Bz) up to 120 °C.

2.3. Binding kinetics and binding efficiency of biotinylated polymeric micelles to streptavidin-coated magnetic beads

To determine the binding kinetics of biotinylated micelles on

streptavidin-coated magnetic beads, nine aliquots of 13 μL of biotinylated micelles labeled with Cy3 (prepared as described in section 2.2; weight fraction of biotinylated polymer was 10%), corresponding to nine different time points, were mixed with 55 μL prewashed beads suspension dispersed in 117 μL of PBS resulting in a molar ratio of streptavidin/biotin (S/B) of 1.3:1. Nonbiotinylated micelles were used to study possible nonspecific binding to the beads. Subsequently, the mixtures were incubated under constant agitation for 0.5 (set as 100% fluorescence signal), 5, 10, 20, 30, 60, 120, 240, and 960 min at 4 °C. The incubation temperature was chosen to avoid any preliminary drug release from the micelles. Next, the samples were placed in a magnetic rack for 1 min resulting in forced sedimentation of the beads. The supernatants were collected and diluted with DMF (1:1, v/v) for fluorescence measurement with excitation and emission wavelengths of 555 and 570 nm, respectively (model FP-8300, JASCO, Hachioji-shi, Tokyo, Japan). To the bead fractions, 130 μL of DMF was added to destabilize the captured biotinylated micelles, and an equal volume of PBS was added prior to fluorescence measurement. The Cy3 fluorescence signals in the supernatant and the bead fraction were taken as the amount of the unbound and bound micelles, respectively. A calibration curve was obtained by diluting Cy3-labeled biotinylated micelles in DMF/PBS (1:1, v/v) at concentrations between 10 and 400 μg/mL.

To determine the binding efficiency of biotinylated micelles to streptavidin-coated magnetic beads, nine aliquots of 13 μL of Cy3-labeled micelles with different weight fractions of the biotinylated block copolymers (0, 2.5, 5, 10, 15, and 20%, respectively), corresponding to nine different amount of beads in the tubes, were mixed with 0 (set as 100% fluorescence signal), 5, 15, 25, 35, 45, 55, 65, and 75 μL prewashed beads suspension in 117 μL of PBS, corresponding to molar ratios of streptavidin/biotin ranging from 0 to 7, respectively, followed by incubation under constant agitation for 10 min at 4 °C. Subsequently, the different samples were placed in a magnetic rack for 1 min, and the amount of free and captured biotinylated micelles was determined by fluorescence measurement of the supernatant and beads fraction.

2.4. In vitro drug release from biotinylated polymeric micelles associated with streptavidin-coated magnetic beads

The release study was conducted using drug-loaded biotinylated micelles in five different media, namely PBS, PBS containing 2% v/v Tween 80, PBS containing 4.5% *w/v* fatty acid-free BSA, mouse plasma, and whole mouse blood. Tween 80 is a surfactant that can solubilize the released compound and therefore act as a sink for hydrophobic compounds in aqueous environments. PTX solubility in PBS containing 2% v/v Tween 80 was reported to be 70 μg/mL (>210× the solubility in PBS) [26], whereas curcumin solubility in PBS/2% v/v Tween 80 was measured to be 28 μg/mL (>2500× solubility in PBS) [27]. In the release assay, the selected volume of PBS/2% Tween 80 (240 μL for 10% drug feed) was sufficient to solubilize the entire dose of PTX (4.8 ± 0.1 μg) and curcumin (4.9 ± 0.1 μg) present in the micellar formulation. Albumin is a transporter/solubilizer for a great variety of both endogenous ligands such as fatty acids and drugs including paclitaxel and curcumin [28–30], and therefore fatty acid-free BSA was used to solubilize the released drug and thus maintain sink conditions. Since one albumin contains two PTX/curcumin-binding sites [29,31], the molar ratio of albumin/drug used in this assay was more than sufficient to solubilize the dose of drug initially present in the micelles (Table S2).

The release of the drugs was studied as follows: 9 aliquots of 13 μL of drug-loaded micelles containing 10% biotinylated polymers (3 or 10% PTX feed, or 10% curcumin feed), corresponding to nine different time points, were mixed with 55 μL prewashed beads which were dispersed in 117 μL of PBS (Fig. 2). After constant agitation for 10 min at 4 °C, the tubes were placed in a magnetic rack for 1 min causing the beads to move to one side of the Eppendorf tubes. The supernatants, possibly containing non-bound micelles and non-encapsulated drugs, were discarded. Predetermined volumes of release medium PBS, PBS/Tween 80, PBS/BSA, mouse plasma, and whole mouse blood (240 μL for 10% drug feed, 130 μL for 3% drug feed) were added to the beads and the samples were subsequently incubated at 37 °C under constant agitation. After 0.5 (set as 100% drug content), 15, 30, 60, 120, 240, 360, 1440, and 2880 min, sample tubes were placed in a magnet rack for 1 min. The supernatants containing the released drug were collected and diluted with ACN (1:1, v/v). In the case of serum protein-containing media (PBS/BSA, mouse plasma, and mouse blood), the precipitated albumin and/or other plasma proteins were centrifuged at 12000 *g* for 10 min prior to HPLC analysis. The method was validated by spiking PBS/BSA, mouse plasma, and whole mouse blood with known amounts of drugs, followed by precipitation of proteins and determination of the amounts of drugs in the supernatants. Full recovery of the added drug was achieved in all media (Table S3). Next, 130 μL of ACN was added to the bead fractions containing the bound micelles plus their retained drug content, to destabilize the micelles. Finally, the drug concentrations were quantified by HPLC analysis. The amounts of drugs in the release media and the bead fractions were taken as the percentage of drug release and drug retention, respectively. The HPLC methods for the detection and quantification of paclitaxel and curcumin can be found in the SI. Each experiment was repeated three times and data are given as the average values based on these three independent measurements.

3. Results and discussion

3.1. Characterization of empty and drug-loaded biotinylated polymeric micelles

Empty biotinylated micelles were prepared by solvent extraction using DMF as a solvent for p(HPMAm)-b-p(HPMAm-Bz) with or without biotin at the p(HPMAm) terminus and water as non-solvent. Table 1 shows that the hydrodynamic diameter of the obtained micelles containing different percentages of the biotinylated polymer ranged between 62 and 77 nm with a low polydispersity (PDI ≤ 0.14), demonstrating a small size distribution. The micelles had a negative zeta potential at pH = 7.4, which is attributed to the carboxylic acid group at the terminal end of the polymer chains that is deprotonated at the measurement conditions (pH = 7.4, Fig. S2). The zeta potential of the micelles became less negative from −16.2 ± 0.5 to −9.0 ± 0.7 mV with an increasing weight fraction of biotinylated block copolymer from 0 to 20%, which most likely can be ascribed to the loss of carboxyl groups upon biotinylation.

Table 2 shows that 10% biotinylated micelles loaded with different feeds of either PTX or curcumin exhibited similar sizes and polydispersity (~65 nm with PDI ≤ 0.14). The micelles showed good encapsulation efficiency (79 ± 4%) and loading capacity (2.6 ± 0.1%) at 3% feed of PTX, whereas the encapsulation efficiency was 51 ± 1% at 10% PTX feed, resulting in a loading capacity of 6.1 ± 0.1%. On the

Table 1
Physicochemical characteristics of empty micelles.[a]

Weight fraction of biotinylated block copolymer (%)	Z_{ave} (nm)	PDI	Zeta potential (mV)
0	70 ± 3	0.13 ± 0.02	−16.2 ± 0.5
2.5	63 ± 5	0.14 ± 0.01	−14.2 ± 0.3
5	62 ± 6	0.14 ± 0.01	−14.0 ± 0.1
10	65 ± 2	0.13 ± 0.01	−13.9 ± 0.2
15	77 ± 4	0.10 ± 0.01	−12.9 ± 0.4
20	75 ± 6	0.13 ± 0.01	−9.0 ± 0.7

[a] Data are presented as mean ± SD of three independently prepared batches.

Table 2
Physicochemical characteristics of drug-loaded biotinylated micelles.[a]

Drug and feed	Z_{ave} (nm)	PDI	EE (%)	LC (%)
PTX, 3%	65 ± 1	0.10 ± 0.01	79 ± 4	2.6 ± 0.1
PTX, 10%	65 ± 5	0.14 ± 0.01	51 ± 1	6.1 ± 0.1
Curcumin, 10%	62 ± 1	0.09 ± 0.01	82 ± 6	9.0 ± 0.1

[a] Data are presented as mean ± SD of three independently prepared batches.

other hand, curcumin was more efficiently loaded in the core of the biotinylated micelles at 10% feed with a high encapsulation efficiency (82 ± 6%) and a loading capacity of 9.0 ± 0.1%. These results are in line with previous studies, in which PTX and curcumin were loaded with high encapsulation efficiency into structurally related micelles based on poly(ethylene glycol)-b-p(HPMAm-Bz) polymers [6,19,32,33].

3.2. Binding properties of biotinylated polymeric micelles

The binding kinetics and binding efficiency of Cy3-labeled biotinylated polymeric micelles with streptavidin-coated magnetic beads were investigated. Our previous study revealed the binding ability of the micelles containing 10% biotinylated polymers by cells that overexpress biotin receptors [21], demonstrating that the biotin groups are exposed at the p(HPMAm) shell of the micelles. Therefore, as expected and shown in Fig. 1A, biotinylated micelles also bound to the streptavidin-coated beads and reached equilibrium within 10 min. This resulted in binding of 90 ± 6% micelles at a molar ratio of streptavidin/biotin (S/B) 1.3:1. Importantly, nonbiotinylated micelles did not show any affinity for the beads upon incubation up to 960 min under the same conditions (Fig. S3), nor with increasing amount of streptavidin beads (Fig. S4), confirming that observed binding of the biotinylated micelles indeed occurred through biotin-streptavidin interactions.

Previous publications have demonstrated that <25% biotin coverage of the surface of polymeric micelles exhibited good surface accessibility and efficient cellular uptake through binding to the biotin receptor [34–37]. Therefore, the weight fraction of biotinylated polymer in the Cy3-labeled micelles was tuned from 2.5 to 20%. Fig. 1B shows that the amounts of bound micelles increased with increasing amounts of beads added to a fixed concentration of micelles. Surprisingly, this was independent of the degree of biotinylation. As shown in Fig. 1C, S/B was linearly related to $1/f$, in which f is the fraction of biotinylated polymers in micelles. As pointed out in section 2 in the Supporting Information, this corresponds to a model in which the surface coverage of the beads by the micelles is indeed independent of the percentage of biotin on the micelles. According to this model, the molar ratio of streptavidin to biotin (S/B) was 0.11. Sleiman et al. reported the application of streptavidin-coated magnetic beads in the quantification of biotin accessibility on the surface of PEGylated luminescent iridium micelles [38]. In their study, a biotinylated PEG-based triblock copolymer was synthesized, and each polymer has on average one biotin unit at the terminal end and thus these micelles were composed of 100% biotinylated polymers. In that case, 24 μg of biotinylated triblock polymer (M_n 20,400) was bound to 1 mL beads (1 mg/mL, containing 0.125 μM streptavidin). Therefore, 1.18 nmol biotinylated polymer (or biotin) was bound to 0.125 nmol streptavidin. The experimental S/B ratio was

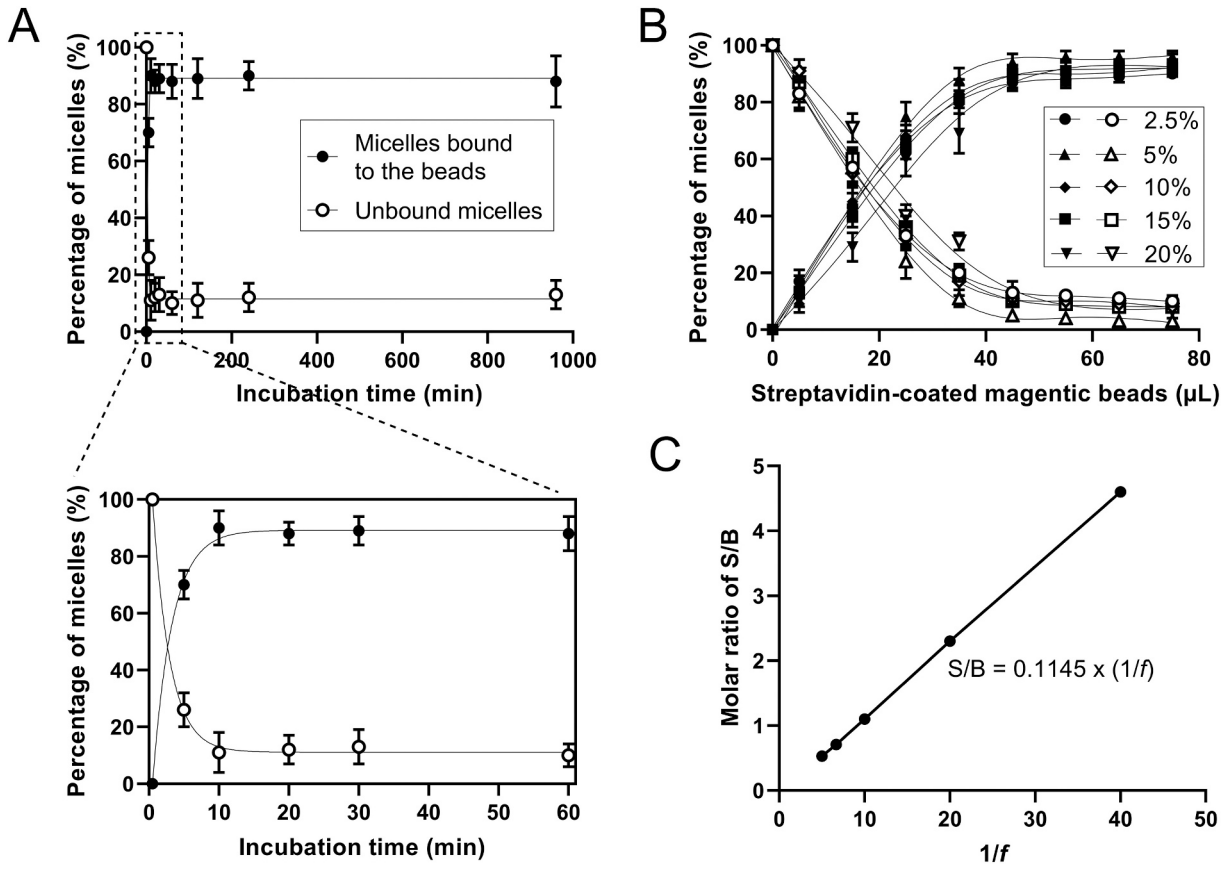

Fig. 1. Binding of biotinylated micelles to streptavidin-coated magnetic beads. (A) Binding kinetics of micelles (with 10% biotinylated polymers) at 4 °C in PBS at S/B = 1.3:1 mol/mol. Data are presented as mean ± SD of three independent replicates. (B) Binding efficiency of micelles upon incubation with increasing volume of streptavidin-coated magnetic beads (added from a stock solution 5 mg/mL) for 10 min at 4 °C in 117 μL PBS. The concentration of micelles was constant, whereas the weight fractions of biotinylated block copolymer were varied. Closed symbols represent the percentage of biotinylated micelles bound to the beads, and open symbols represent the percentage of unbound micelles. (C) The molar ratio of streptavidin/biotin (S/B) as a function of $1/f$, where f is the fraction of biotinylated polymers in micelles.

0.125/1.18 = 0.11, which is in excellent agreement with our value. In our study, the number of streptavidin units that are covered by each micelle is equal to 0.11 × N_{agg} = ~90, assuming an aggregation number (N_{agg}) of 800 [22]. The surface of a projected circle with a diameter of 70 nm is 3848 nm^2 which covers those 90 streptavidin molecules, which in turn equals ~42 nm^2 per streptavidin molecule assuming that the surface of the beads is fully covered with streptavidin. This corresponds to a diameter of 7.3 nm for one streptavidin molecule, which is close to the previously reported size of streptavidin (4.2 × 4.2 × 5.6 nm) [39].

3.3. Drug release from biotinylated polymeric micelles

To confirm that polymeric micelles do not dissociate in the release media nor fuse with components of the media, PBS, PBS containing 2% v/v Tween 80, and 4.5% *w/v* fatty acid-free BSA were incubated with drug-loaded biotinylated micelles at 37 °C for 48 h. The size of micelles was not changed as measured by DLS and Tween micelles (± 20 nm) and BSA (± 6 nm) were detected as separate peaks (Fig. S5). As shown in Fig. 2, the drug-loaded micelles were pre-captured by the beads after incubation at 4 °C for 10 min in PBS and subsequent collection by a magnetic rack. PBS was then discarded to remove non-encapsulated drug molecules or loosely bound drug-loaded micelles. The PTX and curcumin in the micelles captured by the beads was 90 ± 3% and 89 ± 3% of the initially loaded drug, respectively (Fig. S6), which is consistent with the binding efficiency of micelles to the beads (Fig. 1A). For the release studies, the captured beads containing drug-loaded micelles were resuspended in the release medium and incubated at 37 °C under constant agitation for 48 h.

3.3.1. Release of PTX from biotinylated polymeric micelles

Upon incubation in PBS, the amount of PTX retained in the micelles first dropped during the first 6 h to 82 and 65%, for micelles with 3 or 10% PTX feed, respectively, followed by a slight decrease reaching 72 and 56% after 48-h incubation, respectively (Fig. 3A). After the first 2 h, the release medium contained 15–20% of the loaded PTX, and thereafter no further increase was observed for the micelles with both 3 and 10% PTX feed. This resulted in a mass balance, which is the sum of released and retained drug, of 70–90% which can likely be ascribed to PTX degradation in the release medium. Representative HPLC chromatograms of free and encapsulated PTX in micelles incubated in PBS/BSA are shown in Fig. S7. Indeed, we found a major degradation peak in the HPLC chromatogram (retention time 6.5 min, UV 227 nm) of released PTX, whereas PTX that was retained in the polymeric micelles was degraded to a lesser extent at the same time interval. This demonstrates that the drug loaded in the hydrophobic core is less degraded than that in the solution, which has been reported previously for other combinations of drugs and polymeric micelles [40–42]. Different from the ~20% PTX release in PBS observed in the current study, it was reported that only 8% of PTX release was observed for mPEG-b-p(HPMAm-Bz) micelles after 48 h incubation in PBS using a centrifugation method [33], supporting that this centrifugation method gives an underestimation of drug release. The novel drug release model can benefit from a dual-parameter metric, *i.e.*, drug release and drug retention. Although the released PTX undergoes degradation in PBS, an accurate release profile can be provided by measuring the drug retention. Moreover, our release method provides additional parameter, *i.e.*, the rate of drug degradation in release medium, which could be useful information in nano-formulation design and application.

As shown in Fig. 3B, 80% of the loaded PTX was released in the medium during the first 4 h incubation in PBS buffer containing 2% v/v Tween 80 as a solubilizer. Thereafter the micelles only showed a slow release of about 2% during the next 44 h. Analysis of the micelles showed that the remaining ~20% of loaded drugs was detected in the micelles, indeed meaning that the mass balance was around 100%. Compared to our novel release approach, the conventional dialysis method showed similar fast PTX release from π- π stacking polymeric micelles during the first 2 h incubation in PBS/Tween 80 or PBS/Triton X-100, which was followed by a gradual release during the following 7 days [6,43]. As the released PTX does not undergo degradation in PBS/Tween, drug release profile can be accurately obtained from the dual parameter of drug release and retention. Fig. 3B also shows that the observed fast release was independent of the initial drug loading. Similar observations have been previously reported for other PTX formulations upon incubation in PBS/Tween 80 [6,44].

A release of 20–25% of the loaded PTX was seen during the first 4–6 h of incubation of the micelles in PBS containing 4.5% *w/v* BSA and thereafter further release was hardly observed (Fig. 3C). The same figure also shows that around 65% of PTX loading was retained in the micelles after 4–6 h of incubation. Our novel release method showed a similar PTX release profile from π- π stacking polymeric micelles in PBS/BSA as

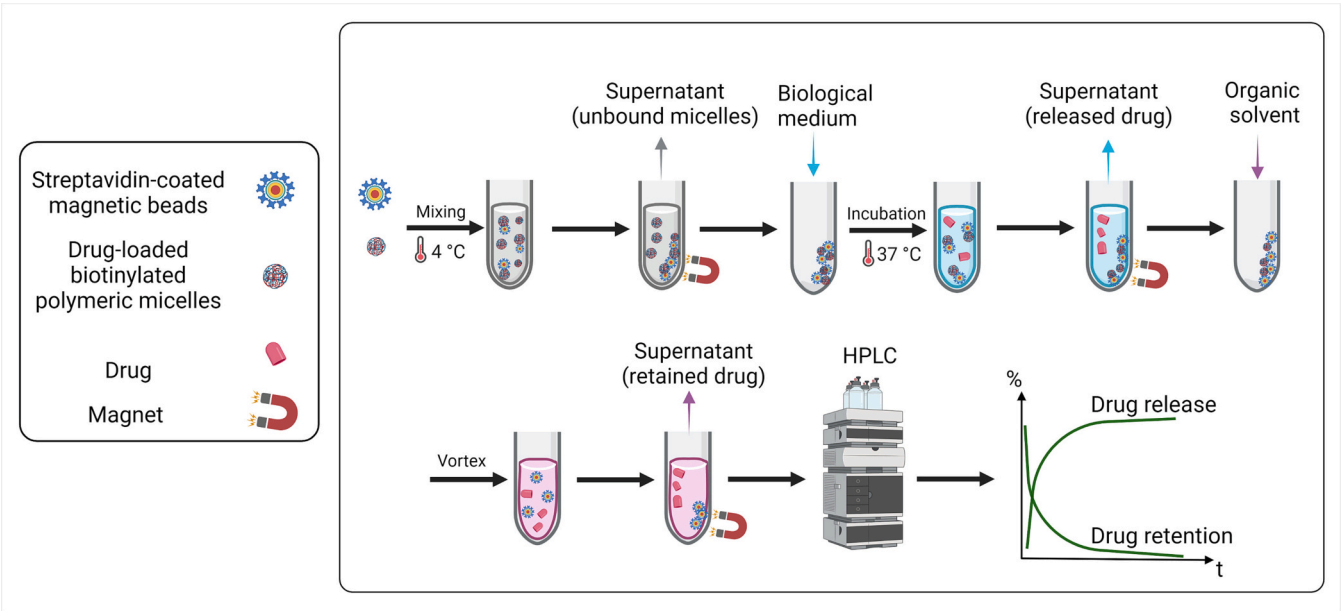

Fig. 2. Schematic illustration of the developed method to study *in vitro* drug release of drugs from polymeric micelles in complex biological media, using biotinylated micelles and streptavidin-coated magnetic beads. The figure was created using BioRender (https://biorender.com/).

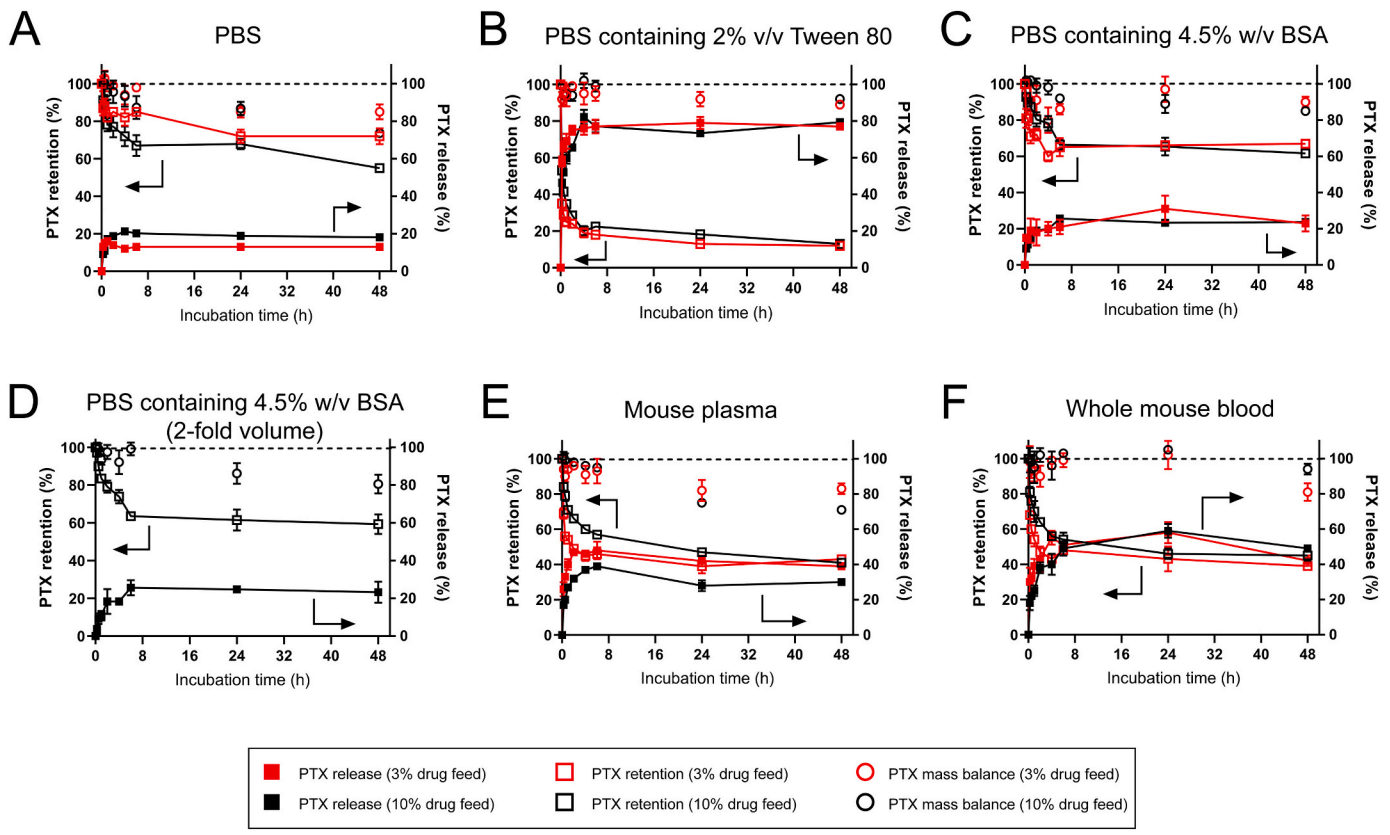

Fig. 3. PTX release and retention profiles. Released and retained PTX were measured (as schematically shown in Fig. 2) by capturing drug-loaded biotinylated micelles with streptavidin-coated magnetic beads from various media upon incubation at 37 °C under constant agitation (in 240 μL medium for 10% PTX feed, 130 μL for 3% PTX feed): (A) PBS, (B) PBS containing 2% v/v Tween 80, (C) PBS containing 4.5% w/w BSA, (D) PBS containing 4.5% w/w BSA (2-fold higher volume), (E) mouse plasma, and (F) whole mouse blood. Filled squares represent released PTX, open squares represent retained PTX, and circles represent the total amount of the measured PTX (= released + retained PTX). Red symbols represent micelles with 3% PTX feed; black symbols represent micelles with 10% PTX feed. The left arrow points to PTX retention; the right arrow points to PTX release. Data are presented as mean ± SD of three independent replicates. (For interpretation of the references to colour in this figure legend, the reader is referred to the web version of this article.)

for the conventional dialysis method [6]. Again, the release profile was not dependent on the initial drug loading (3 and 10%). Further, to prove that drug release is release medium volume-independent, a release study was performed with a fixed volume and concentration of micelles (10% PTX loading) using a 2-fold volume of PBS/BSA. As shown in Fig. 3D, the PTX release and retention profiles were within the experimental error like those in a 2-fold smaller volume of PBS/BSA (Fig. 3C), demonstrating that sink conditions were valid at both conditions.

When micelles with 3 and 10% PTX loading were incubated in mouse plasma at 37 °C, the PTX retention decreased to about 50% during the first 6 h, and thereafter gradually decreased to 40% at 48 h. Accordingly, up to 50% of the loaded drug was observed in the release medium during the first 6 h (Fig. 3E). However, during the next 6 to 48 h of incubation, total PTX measured in the medium did not further increase but decreased to 30–45%. Eventually, the total mass balance was around 80% at 48 h for both micelles with 3 and 10% PTX loading, which is likely due to the above-mentioned degradation of PTX.

Fig. 3C and E show that PTX was released faster in mouse plasma than in PBS/BSA. Also, the amount of PTX released is higher in plasma than that in BSA. It has previously been reported that the photosensitizer meta-tetra(hydroxyphenyl)chlorin (mTHPC) was released from benzyl-poly(ε-caprolactone)-b-poly(ethylene glycol) micelles in a medium-dependent manner using asymmetric flow field flow fractionation (AF4) [45]. It was found that the release of mTHPC in human plasma occurred faster and to a higher extent than that in human serum albumin (HSA), likely due to the high affinity of the photosensitizer for specific plasma proteins, *i.e.*, lipoproteins. Kumar et al. reported that, PTX, besides to HSA, also binds to alpha 1-acid glycoprotein and lipoprotein [46]. Therefore, the presence of these proteins in mouse plasma may accelerate PTX release as compared to PBS/BSA as a release medium.

Upon incubation in whole mouse blood, independent of the initial loading, around 50% of the loaded PTX was released from the micelles during the first 6 h, and 40–45% of PTX was retained in the micelles after 48 h incubation, resulting in a mass balance of >90% (Fig. 3F). Hence, very similar PTX retention profiles were observed in whole mouse blood and plasma (Fig. 3E & F). However, the amount of PTX measured in whole blood medium was 1.5-fold higher than that in plasma at 24 h-incubation. This discrepancy of PTX released in plasma and whole blood requires further investigation.

3.3.2. *Release of curcumin from biotinylated polymeric micelles*

Incubation of curcumin-loaded micelles with 10% loading in PBS at 37 °C showed that 50% of the initial amount was still retained in the micelles after 6 h (Fig. 4A). The faster release of curcumin compared to PTX is likely due to less compatibility of curcumin with the hydrophobic core of the micelles. Thereafter the retained curcumin slowly dropped to ~30% during the next 42 h. However, no released curcumin was detected in PBS, resulting in a mass balance of only 30% at 48 h. Given the near insolubility of curcumin in an aqueous solution and poor stability at pH > 6.5 [47–49], it is plausible that the released curcumin was precipitated and/or degraded. Indeed, we did observe curcumin degradation products (UV 254 nm) in the chromatogram with retention times of 1.50–2.20 min after 48-h incubation (Fig. S8), probably including bicyclopentadione as demonstrated by Naksuriya et al. [48].

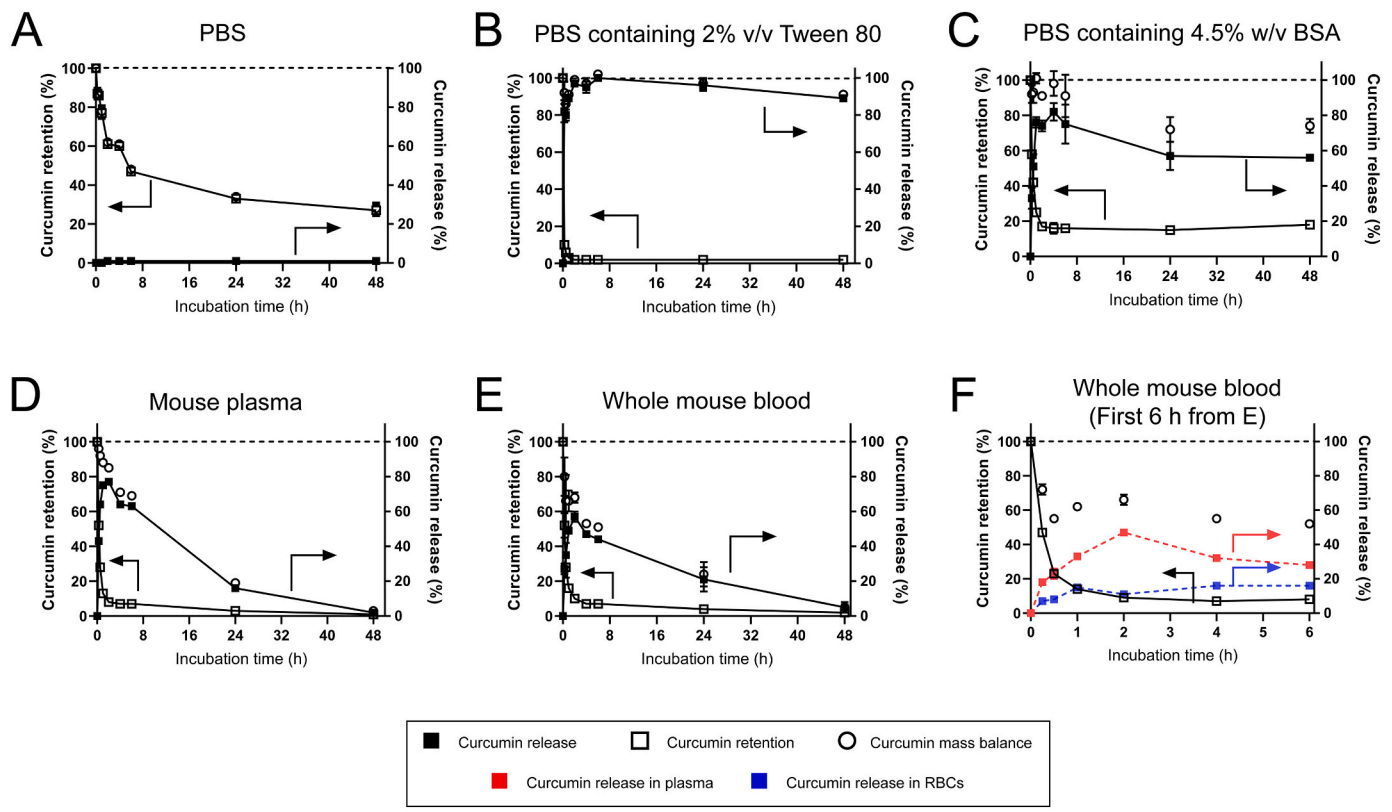

Fig. 4. Curcumin release profiles. Curcumin retention and release were measured in various media by capturing drug-loaded biotinylated micelles with streptavidin-coated magnetic beads upon incubation at 37 °C under constant agitation: (A) PBS, (B) PBS containing 2% v/v Tween 80, (C) PBS containing 4.5% w/w BSA, (D) mouse plasma, (E) whole mouse blood, and (F) first 6 h in whole mouse blood. Filled black squares represent curcumin release, open black squares represent curcumin retention, and black circles represent the total amount of the measured curcumin. The left arrow points to curcumin retention; the right arrow points to curcumin release. Data are presented as mean ± SD of three independent replicates.

When PBS was supplemented with 2% v/v Tween 80, loaded curcumin was quantitatively released in the first hour of incubation, and the mass balance was ~100% (Fig. 4B). Obviously, the Tween micelles solubilized the released curcumin and also protected it against degradation which is in line with our previous findings [48].

Fig. 4C shows that when curcumin-loaded micelles were incubated in PBS containing 4.5% *w/v* BSA, 80% of the loaded curcumin was rapidly released in the first 1–2 h and 20% of loading was retained in the micelles. This graph also shows that micelles did not release the remaining 20% curcumin whereas the released amount gradually dropped from 80% to 60% after 48 h, leading to a mass balance of ~80%. The gradual drop is likely caused by the degradation of the albumin-bound curcumin. Although one albumin molecule can bind two curcumin molecules and protect curcumin against decomposition [19,50], obviously, the protection of curcumin degradation by albumin is inferior to that of Tween micelles (Fig. 4B & C). Fig. 4D shows that incubation of curcumin-loaded micelles at 37 °C in plasma also showed a rapid release in the first 1–2 h of up to 80% of the loading, and the released curcumin was fully degraded within 48 h. Curcumin degradation peaks with retention times of 1.50–2.20 min at UV 254 nm were observed in the HPLC chromatogram. Around 5% of loaded curcumin was retained in the micelles between 2 and 6 h of incubation with plasma and at 48 h no curcumin was detected in the micelles. Finally, during the incubation of curcumin-loaded micelles in whole blood, the same retention profile for curcumin was observed as for plasma (Fig. 4E). It is remarked that the degradation rate of curcumin was faster in whole mouse blood than that in plasma (Fig. 4D & E). By spinning down the blood cells, ~20% of curcumin was observed to be associated with RBCs in the first 6 h-incubation (Fig. 4F), yet the AUC of degradation peaks in RBCs fraction also increased within 6 h. This can be possibly explained by the redistribution of curcumin from the plasma fraction to the RBCs. These results support the instability of curcumin in the presence of albumin and particularly erythrocytes, which is in line with previous reports that curcumin is distributed into, and metabolized by RBCs in a species-dependent manner [51–53]. Our release method provides a useful tool to study the association of released curcumin with erythrocytes, which will provide useful insights for the investigation of the pharmacokinetics and the tissue distribution of curcumin.

These results show that the curcumin release in PBS/Tween > plasma ≈ whole blood > PBS/BSA > PBS within 8 h incubation. The released curcumin was stabilized by albumin to some extent, and a delayed curcumin degradation in PBS/BSA and plasma was seen within 6 h incubation as compared to curcumin released in PBS (Fig. 4A & C), which is in good agreement with a previous publication that the released curcumin from mPEG-b-p(HPMAm-Bz) micelles was subsequently solubilized by albumin as determined by AF4 analysis [19]. Similarly, Wang et al. also reported that curcumin degradation was significantly reduced in cell culture medium containing 10% fetal calf serum and in human blood than in 0.1 M phosphate buffer during 8 h incubation [54]. Kee et al. revealed that albumin and fibrinogen are responsible for binding curcumin in human plasma, and more importantly, these proteins suppress the hydrolysis of curcumin and thus retard degradation [55].

4. Conclusion

A new *in vitro* method for studying the release kinetics of water-insoluble drugs from polymeric micelles in complex biological media is described. The proposed “fishing” approach of biotinylated nanoparticles by streptavidin-coated magnetic beads enables the

determination of time-dependent drug retention and release (and thus total mass balance) in biological media. Moreover, our results illustrate how inappropriate *in vitro* release media, like PBS and PBS supplemented with solubilization agents such as surfactant or BSA, can lead to underestimated or overestimated drug release kinetics and profiles, and result in a misleading conclusion of drug retention. In this work, we demonstrate that this assay allows studying the release of PTX and curcumin from polymeric micelles in mouse plasma and whole mouse blood *in vitro*. Since biotinylated polymers and lipids can be easily synthesized and are also commercially available, this novel method can be extended to other biotinylated nanoformulations in a broad range of biological media *e.g.*, homogenate suspensions of tumor tissues, and loaded with a wide variety of drugs, both of hydrophobic and hydrophilic nature. In conclusion, the further development and application of the magnetic beads-enabled method potentially improves the reliability of the *in vitro* release assay, thereby facilitating high throughput testing of various nanomedicines and reducing the number of animal experiments needed.

Contributions

All authors contributed to the design of experiments, data acquisition, analysis and interpretation, and writing of the manuscript.

Appendix A. Supplementary data

Supplementary data to this article can be found online at https://doi.org/10.1016/j.jconrel.2022.07.044.

References

[1] D. Hwang, J.D. Ramsey, A.V. Kabanov, Polymeric micelles for the delivery of poorly soluble drugs: from nanoformulation to clinical approval, Adv. Drug Deliv. Rev. 156 (2020) 80–118.

[2] A. Varela-Moreira, Y. Shi, M.H.A.M. Fens, T. Lammers, W.E. Hennink, R. M. Schiffelers, Clinical application of polymeric micelles for the treatment of cancer, Mater. Chem. Front. 1 (2017) 1485–1501.

[3] H. Cabral, K. Miyata, K. Osada, K. Kataoka, Block copolymer micelles in nanomedicine applications, Chem. Rev. 118 (2018) 6844–6892.

[4] L. Houdaihed, J.C. Evans, C. Allen, Overcoming the road blocks: advancement of block copolymer micelles for cancer therapy in the clinic, Mol. Pharm. 14 (2017) 2503–2517.

[5] P. Mi, K. Miyata, K. Kataoka, H. Cabral, Clinical translation of self-assembled cancer nanomedicines, Adv. Ther. 4 (2021), e2000159.

[6] M. Sheybanifard, N. Beztsinna, M. Bagheri, E.M. Buhl, J. Bresseleers, A. Varela-Moreira, Y. Shi, C.F. van Nostrum, G. van der Pluijm, G. Storm, W.E. Hennink, T. Lammers, J.M. Metselaar, Systematic evaluation of design features enables efficient selection of Π electron-stabilized polymeric micelles, Int. J. Pharm. 584 (2020), e119409.

[7] A. Ranjan, P.K. Jha, Experiments and modeling of controlled release behavior of commercial and model polymer-drug formulations using dialysis membrane method, Drug Deliv. Transl. Res. 10 (2020) 515–528.

[8] M. Ghezzi, S. Pescina, C. Padula, P. Santi, E. Del Favero, L. Cantù, S. Nicoli, Polymeric micelles in drug delivery: an insight of the techniques for their characterization and assessment in biorelevant conditions, J. Control. Release 332 (2021) 312–336.

[9] M. Yu, W. Yuan, D. Li, A. Schwendeman, S.P. Schwendeman, Predicting drug release kinetics from nanocarriers inside dialysis bags, J. Control. Release 315 (2019) 23–30.

[10] S.A. Abouelmagd, B. Sun, A.C. Chang, Y.J. Ku, Y. Yeo, Release kinetics study of poorly water-soluble drugs from nanoparticles: are we doing it right? Mol. Pharm. 12 (2015) 997–1003.

[11] Council of Europe, Chapter 2.9.3 Dissolution test for solid dosage forms, in: Eur. Pharmacopoeia, 8th ed., EDQM, Strasbourg Cedex, France, 2014.

[12] D.J. Phillips, S.R. Pygall, V.B. Cooper, J.C. Mann, Overcoming sink limitations in dissolution testing: a review of traditional methods and the potential utility of biphasic systems, J. Pharm. Pharmacol. 64 (2012) 1549–1559.

[13] S.C. Wang, T.C. Wei, W. Bin Chen, H.K. Tsao, Effects of surfactant micelles on viscosity and conductivity of poly(ethylene glycol) solutions, J. Chem. Phys. 120 (2004) 4980–4988.

[14] S. Myhre, M. Amann, L. Willner, K.D. Knudsen, R. Lund, How detergents dissolve polymeric micelles: kinetic pathways of hybrid micelle formation in SDS and block copolymer mixtures, Langmuir. 36 (2020) 12887–12899.

[15] S. D'Souza, A review of in vitro drug release test methods for nano-sized dosage forms, Adv. Pharm. 2014 (2014) 1–12.

[16] J. Weng, H.H.Y. Tong, S.F. Chow, In vitro release study of the polymeric drug nanoparticles: development and validation of a novel method, Pharmaceutics. 12 (2020), e732.

[17] Y. Zhao, F. Fay, S. Hak, J. Manuel Perez-Aguilar, B.L. Sanchez-Gaytan, B. Goode, R. Duivenvoorden, C. de Lange Davies, A. Bjørkøy, H. Weinstein, Z.A. Fayad, C. Pérez-Medina, W.J.M. Mulder, Augmenting drug–carrier compatibility improves tumour nanotherapy efficacy, Nat. Commun. 7 (2016), e11221.

[18] V. Gray, S. Cady, D. Curran, J. Demuth, O. Eradiri, M. Hussain, J. Krämer, J. Shabushnig, E. Stippler, D.G. Hunt, In vitro release test methods for drug formulations for parenteral applications, Dissolut. Technol. 25 (2018) 8–13.

[19] M. Bagheri, M.H. Fens, T.G. Kleijn, R.B. Capomaccio, D. Mehn, P.M. Krawczyk, E. M. Scutigliani, A. Gurinov, M. Baldus, N.C.H. van Kronenburg, R.J. Kok, M. Heger, C.F. van Nostrum, W.E. Hennink, In vitro and in vivo studies on HPMA-based polymeric micelles loaded with curcumin, Mol. Pharm. 18 (2021) 1247–1263.

[20] Z.S. Al-Ahmady, M. Hadjidemetriou, J. Gubbins, K. Kostarelos, Formation of protein corona in vivo affects drug release from temperature-sensitive liposomes, J. Control. Release 276 (2018) 157–167.

[21] Y. Wang, M.J. van Steenbergen, N. Beztsinna, Y. Shi, T. Lammers, C.F. van Nostrum, W.E. Hennink, Biotin-decorated all-HPMA polymeric micelles for paclitaxel delivery, J. Control. Release 328 (2020) 970–984.

[22] Y. Wang, D.M.E. Thies-Weesie, E.D.C. Bosman, M.J. van Steenbergen, J. van den Dikkenberg, Y. Shi, T. Lammers, C.F. van Nostrum, W.E. Hennink, Tuning the size of all-HPMA polymeric micelles fabricated by solvent extraction, J. Control. Release 343 (2022) 338–346.

[23] W.X. Ren, J. Han, S. Uhm, Y.J. Jang, C. Kang, J.S.H. Kim, J.S.H. Kim, Recent development of biotin conjugation in biological imaging, sensing, and target delivery, Chem. Commun. 51 (2015) 10403–10418.

[24] S. Kenth, J.P. Sylvestre, K. Fuhrmann, M. Meunier, J.C. Leroux, Fabrication of paclitaxel nanocrystals by femtosecond laser ablation and fragmentation, J. Pharm. Sci. 100 (2011) 1022–1030.

[25] T. Esatbeyoglu, K. Ulbrich, C. Rehberg, S. Rohn, G. Rimbach, Thermal stability, antioxidant, and anti-inflammatory activity of curcumin and its degradation product 4-vinyl guaiacol, Food Funct. 6 (2015) 887–893.

[26] T. Yang, F. De Cui, M.K. Choi, J.W. Cho, S.J. Chung, C.K. Shim, D.D. Kim, Enhanced solubility and stability of PEGylated liposomal paclitaxel: in vitro and in vivo evaluation, Int. J. Pharm. 338 (2007) 317–326.

[27] A. Umerska, C. Gaucher, F. Oyarzun-Ampuero, I. Fries-Raeth, F. Colin, M. G. Villamizar-Sarmiento, P. Maincent, A. Sapin-Minet, Polymeric nanoparticles for increasing oral bioavailability of curcumin, Antioxidants 7 (2018) 1–18.

[28] M.T. Larsen, M. Kuhlmann, M.L. Hvam, K.A. Howard, Albumin-based drug delivery: harnessing nature to cure disease, Mol. Cell. Ther. 4 (2016) 1–12.

[29] K. Paál, J. Müller, L. Hegedûs, High affinity binding of paclitaxel to human serum albumin, Eur. J. Biochem. 268 (2001) 2187–2191.

[30] T. Kar, P. Basak, S. Sen, R.K. Ghosh, M. Bhattacharyya, Analysis of curcumin interaction with human serum albumin using spectroscopic studies with molecular simulation, Front. Biol. (Beijing) 12 (2017) 199–209.

[31] A. Barik, B. Mishra, A. Kunwar, K. Indira Priyadarsini, Interaction of curcumin with human serum albumin: thermodynamic properties, fluorescence energy transfer and denaturation effects, Chem. Phys. Lett. 436 (2007) 239–243.

[32] Y. Shi, M.J. Van Steenbergen, E.A. Teunissen, L. Novo, S. Gradmann, M. Baldus, C. F. Van Nostrum, W.E. Hennink, Π-Π stacking increases the stability and loading capacity of thermosensitive polymeric micelles for chemotherapeutic drugs, Biomacromolecules 14 (2013) 1826–1837.

[33] Y. Shi, R. Van Der Meel, B. Theek, E. Oude Blenke, E.H.E. Pieters, M.H.A.M. Fens, J. Ehling, R.M. Schiffelers, G. Storm, C.F. Van Nostrum, T. Lammers, W.E. Hennink, Complete regression of xenograft tumors upon targeted delivery of paclitaxel via Π-Π stacking stabilized polymeric micelles, ACS Nano 9 (2015) 3740–3752.

[34] J. Jin, D. Wu, P. Sun, L. Liu, H. Zhao, Amphiphilic triblock copolymer bioconjugates with biotin groups at the junction points: synthesis, self-assembly, and bioactivity, Macromolecules. 44 (2011) 2016–2024.

[35] X. Wang, L. Liu, Y. Luo, H. Zhao, Bioconjugation of biotin to the interfaces of polymeric micelles via in situ click chemistry, Langmuir. 25 (2009) 744–750.

[36] K. Qi, Q. Ma, E.E. Remsen, C.G. Clark, K.L. Wooley, Determination of the bioavailability of biotin conjugated onto shell cross-linked (SCK) nanoparticles, J. Am. Chem. Soc. 126 (2004) 6599–6607.

[37] A. Doerflinger, N.N. Quang, E. Gravel, G. Pinna, M. Vandamme, F. Ducongé, E. Doris, Biotin-functionalized targeted polydiacetylene micelles, Chem. Commun. 54 (2018) 3613–3616.

[38] K.L. Metera, K.D. Ha-nni, G. Zhou, M.K. Nayak, H.S. Bazzi, D. Juncker, H. F. Sleiman, Luminescent iridium(III)-containing block copolymers: self-assembly into biotin-labeled micelles for biodetection assays, ACS Macro Lett. 1 (2012) 954–959.

[39] E.H. Williams, A.V. Davydov, A. Motayed, S.G. Sundaresan, P. Bocchini, L. J. Richter, G. Stan, K. Steffens, R. Zangmeister, J.A. Schreifels, M.V. Rao, Immobilization of streptavidin on 4H-SiC for biosensor development, Appl. Surf. Sci. 258 (2012) 6056–6063.

[40] M. Elsabahy, M.É. Perron, N. Bertrand, G.E. Yu, J.C. Leroux, Solubilization of docetaxel in poly(ethylene oxide)-block-poly(butylene/styrene oxide) micelles, Biomacromolecules. 8 (2007) 2250–2257.

[41] A. Kara, N. Ozturk, G. Esendagli, U.U. Ozkose, S. Gulyuz, O. Yilmaz, D. Telci, A. Bozkir, I. Vural, Development of novel self-assembled polymeric micelles from partially hydrolysed poly(2-ethyl-2-oxazoline)-co-PEI-b-PCL block copolymer as non-viral vectors for plasmid DNA in vitro transfection, Artif. Cells Nanomed. Biotechnol. 46 (2018) S264–S273.

[42] M.S. Alai, W.J. Lin, S.S. Pingale, Application of polymeric nanoparticles and micelles in insulin oral delivery, J. Food Drug Anal. 23 (2015) 351–358.

[43] A. Varela-moreira, H. Van Leur, D. Krijgsman, V. Ecker, M. Braun, M. Buchner, M. H.A.M. Fens, W.E. Hennink, M. Schiffelers, Utilizing in vitro drug release assays to predict in vivo drug retention in micelles, Int. J. Pharm. 618 (2022), 121638.
[44] Y. Wei, Z. Xue, Y. Ye, Y. Huang, L. Zhao, Paclitaxel targeting to lungs by way of liposomes prepared by the effervescent dispersion technique, Arch. Pharm. Res. 37 (2014) 728–737.
[45] Y. Liu, M.H.A.M. Fens, R.B. Capomaccio, D. Mehn, L. Scrivano, R.J. Kok, S. Oliveira, W.E. Hennink, C.F. van Nostrum, Correlation between in vitro stability and pharmacokinetics of poly(ε-caprolactone)-based micelles loaded with a photosensitizer, J. Control. Release 328 (2020) 942–951.
[46] G.N. Kumar, U.K. Walle, K.N. Bhalla, T. Walle, Binding of taxol to human plasma, albumin and alpha 1-acid glycoprotein, Res. Commun. Chem. Pathol. Pharmacol. 80 (1993) 337–344.
[47] M. Kharat, Z. Du, G. Zhang, D.J. McClements, Physical and chemical stability of curcumin in aqueous solutions and emulsions: impact of pH, temperature, and molecular environment, J. Agric. Food Chem. 65 (2017) 1525–1532.
[48] O. Naksuriya, M.J. Vansteenbergen, J.S. Torano, S. Okonogi, W.E. Hennink, A kinetic degradation study of curcumin in its free form and loaded in polymeric micelles, AAPS J. 18 (2016) 777–787.
[49] M. Heger, R.F. van Golen, M. Broekgaarden, M.C. Michel, The molecular basis for the pharmacokinetics and pharmacodynamics of curcumin and its metabolites in relation to cancers, Pharmacol. Rev. 66 (2014) 222–307.
[50] A. Basu, G. Suresh Kumar, Elucidating the energetics of the interaction of non-toxic dietary pigment curcumin with human serum albumin: a calorimetric study, J. Chem. Thermodyn. 70 (2014) 176–181.
[51] G.T. Bolger, A. Licollari, A. Tan, R. Greil, B. Vcelar, M. Majeed, L. Helson, Distribution and metabolism of lipocurcTM (liposomal curcumin) in dog and human blood cells: species selectivity and pharmacokinetic relevance, Anticancer Res. 37 (2017) 3483–3492.
[52] A. Storka, B. Vcelar, L. Helson, M. Wolzt, PP119—effect of liposomal curcumin on red blood cells in vitro, Clin. Ther. 35 (2013), e52.
[53] M.M. Yallapu, M.C. Ebeling, N. Chauhan, M. Jaggi, S.C. Chauhan, Interaction of curcumin nanoformulations with human plasma proteins and erythrocytes, Int. J. Nanomedicine 6 (2011) 2779–2790.
[54] Y.J. Wang, M.H. Pan, A.L. Cheng, L.I. Lin, Y.S. Ho, C.Y. Hsieh, J.K. Lin, Stability of curcumin in buffer solutions and characterization of its degradation products, J. Pharm. Biomed. Anal. 15 (1997) 1867–1876.
[55] M.H.M. Leung, T.W. Kee, Effective stabilization of curcumin by association to plasma proteins: human serum albumin and fibrinogen, Langmuir. 25 (2009) 5773–5777.